

The central region of CNOT1 and CNOT9 stimulate deadenylation by the Ccr4-Not nuclease module

Lorenzo Pavanello^{1,#}, Benjamin Hall¹, Blessing Airhihen^{1,%}, and Gerlof Sebastiaan Winkler^{1,*}

¹ School of Pharmacy, University of Nottingham, East Drive, University Park, Nottingham NG7 2RD, U.K.

* Author for correspondence:

Tel: +44-115-8468457

Email:sebastiaan.winkler@nottingham.ac.uk

Present address:

Domainex Ltd, Chesterford Research Park, Little Chesterford, Saffron Walden, Essex CB10 1XL, U.K.

% Permanent address:

School of Pharmacy, Pharmacology Department, Niger Delta University, Wilberforce Island, Amassoma, Bayelsa state, Nigeria

Keywords:

Ribonuclease; Deadenylase; Caf1/CNOT7; Mg²⁺ dependent enzyme; RNA; RQCD-1; Protein expression

Abstract

Regulated degradation of cytoplasmic mRNA is important for the accurate execution of gene expression programmes in eukaryotic cells. A key step in this process is the shortening and removal of the mRNA poly(A) tail, which can be achieved by the recruitment of the multi-subunit Ccr4-Not nuclease complex *via* sequence-specific RNA binding proteins or the microRNA machinery. The Ccr4-Not complex contains several modules that are attached to its large subunit CNOT1. Modules include the nuclease module, which associates with the MIF4G domain of CNOT1 and contains the catalytic subunits Caf1 and Ccr4, as well as the module containing the non-catalytic CNOT9 subunit, which binds to the DUF3819 domain of CNOT1. To understand the contributions of the individual modules to the activity of the complex, we have started to reconstitute sub-complexes of the human Ccr4-Not complex containing one or several functional modules. Here, we report the reconstitution of a pentameric complex including a BTG2-Caf1-Ccr4 nuclease module, CNOT9 and the central region of CNOT1 encompassing the MIF4G and DUF3819 domains. By comparing the biochemical activities of the pentameric complex and the nuclease module, we conclude that the CNOT1-CNOT9 components stimulate deadenylation by the nuclease module. In addition, we show that a pentameric complex containing the melanoma-associated CNOT9 P131L variant is able to support deadenylation similar to a complex containing the wild type CNOT9 protein.

Introduction

Regulated degradation of cytoplasmic mRNA is essential for the control of gene expression programmes in eukaryotic cells [1-3]. Control of mRNA decay typically involves the recognition of sequence elements in the 3' untranslated region of mRNAs by RNA-binding proteins or miRNA-mediated repression complexes, which recruit components of the RNA-degradation machinery [4-6]. Decay is initiated by shortening and removal of the poly(A) tail via the enzymatic action of the Ccr4-Not and Pan2-Pan3 deadenylases. Subsequently, the 5' cap structure of the mRNA is removed, followed by 5'-3' degradation by the exonuclease Xrn1 or 3'-5' degradation by the exosome complex [1-3, 5]. In recent years, an expanding number of RNA-binding factors have been identified that specifically interact with the Ccr4-Not complex, which appears to be a focal point of regulated mRNA degradation. Examples include the PUF proteins [7], Nanos [8, 9] and Tristetraprolin (TTP; zinc-finger protein ZFP36) [10-12], which are sequence-specific RNA-binding proteins; Roquin, which binds to a stem-loop structural element [13, 14]; and GW182 (TNRC6), which is a core component of the miRNA-repression complex [15, 16].

Ccr4-Not is a large multi-subunit complex composed of eight subunits with the large subunit CNOT1 acting as a scaffold for different functional modules [6, 17]. The N-terminal domain is bound by CNOT10 and CNOT11 [18, 19], while the C-terminal region forms the NOT module with the CNOT2 and CNOT3 subunits [20, 21]. The central region of CNOT1 encompasses two domains. The MIF4G domain mediates interactions with the two catalytic subunits of the complex: Caf1, a DEDDh-type ribonuclease, and Ccr4, which contains an EEP (Endonuclease-Exonuclease-Phosphatase) domain [22, 23]. The contribution of each of the catalytic subunits to the activity of the Ccr4-Not complex appears to differ in various organisms. In the yeast *Saccharomyces cerevisiae*, the active site of Caf1 contains non-conserved amino acids at key positions and its activity is not required for its *in vivo* function [24]. By contrast, the Caf1 and Ccr4 subunits both contribute to the activity of the purified *Schizosaccharomyces pombe* complex or the *Drosophila melanogaster* nuclease module [25, 26]. Interestingly, the activities of Caf1 and Ccr4 are both required for the activity of the human nuclease module and inactivating mutations in the active site of either Caf1 or Ccr4 abolish all activity of the nuclease module [27]. Adjacent to the MIF4G domain is the DUF3819 domain (domain of unknown function 3819), which provides a platform for CNOT9 (RQCD1/Caf40) [15, 16]. The latter can mediate interactions with RNA-binding factors, including the miRNA-associated protein GW182 [15, 16], the ARE (A/U rich element) binding protein TTP [11], and the stem-loop binding protein Roquin [13]. A recurrent mutation in CNOT9 resulting in amino acid change P131L is found in a sub-set of melanoma tumours, but the impact of this amino acid substitution on the structure and function of CNOT9 is currently unknown [28].

It is unclear whether the non-catalytic subunits have roles other than mediating protein-protein interactions with RNA-binding regulatory factors. It has been reported that an intact recombinant *S. pombe* Ccr4-Not complex has greater deadenylase activity than the isolated nuclease module, but it is not known which components contribute to the stimulation of the nuclease subunits [26]. To begin to address this question, we aimed to reconstitute functional Ccr4-Not sub-complexes containing one or several functional modules. To this end, we recently reported the initial reconstitution of a trimeric nuclease sub-complex composed of human BTG2-Caf1-Ccr4 [27]. To extend this approach and begin to evaluate the contribution of the non-catalytic subunits of Ccr4-

Not to deadenylation, we aimed to expand the nuclease module by including the central region of CNOT1 encompassing the MIF4G and DUF3819 domains as well as the CNOT9 subunit. Analysis of the deadenylase activities of this pentameric sub-complex, which we termed the central module, revealed a role for the non-catalytic subunits in stimulating the enzymatic activity of the nuclease module. In addition, we show that the central module containing the melanoma-associated CNOT9 P131L variant is able to support deadenylation similar to a complex containing wild type CNOT9.

Experimental

Expression and purification of Caf1 and the BTG2-Caf1 dimer

The monomeric human Caf1/CNOT7 enzyme was expressed and purified from *Escherichia coli* BL21 (DE3) using expression plasmid pQE80L-CNOT7 as described before [29]. The catalytically inactive version containing the amino acid substitution D40A was also expressed and purified as described before [29].

The BTG2-Caf1/CNOT7 dimer was expressed and purified as described before [27], except that a vector for dual expression of BTG2 and Caf1 was used. Plasmid pACYC-Duet1-BTG2/CNOT7 was generated for dual expression of His-BTG2 and Caf1/CNOT7. Briefly, a codon-optimised CNOT7 cDNA (digested with 5' BamHI and 3' SalI) was inserted in the BglII and XhoI restriction sites of multiple cloning site 2 of vector pACYC-Duet1 (Merck). Then, the human BTG2 cDNA was inserted into multiple cloning site 1 using the BamHI and HindIII restriction sites. The BTG2-Caf1 dimer was subsequently expressed and purified as described before [27]. Purified proteins were stored in small aliquots at -80°C. Protein concentrations were determined using the Protein Assay Reagent (Bio-Rad).

Expression and purification of the trimeric BTG2-Caf1-Ccr4 nuclease module

The trimeric BTG2-Caf1-Ccr4 complex was purified using a modified two-step procedure by co-expression of BTG2, Strep-Ccr4/CNOT6L, and Caf1/CNOT7 [27].

Plasmid pACYC-Duet1-Strep-CNOT6L/CNOT7 for dual expression of Strep-tagged CNOT6L and CNOT7 was generated in two stages. First, the pQE80L expression vector (Qiagen) was modified by replacing the His-tag coding sequences with Strep-tag coding sequences by inserting a synthetic duplex formed by oligonucleotides 5'- AATTCA-TTAAAGAGGAGAAATTAATACTATGGCTAGCTGGAGCCACCCGCAGTTCGAGAAAGGTGGAGGTT-CCGGAGGTGGATCGGGAGGTGGATCGTGGAGCCACCCGCAGTTCGAAAAAG -3' and 5'-GAT-CCTTTTTTCGAACTGCGGGTGGCTCCACGATCCACCTCCCGATCCACCTCCGGAACCTCCACCTT-TCTCGAACTGCGG-GTGGCTCCAGCTAGCCATAGTTAATTTCTCCTTTTAATG-3' into the 5' EcoRI and 3' BamHI restriction sites of pQE80L. Then, a codon-optimised CNOT6L cDNA was inserted into the 5' BamHI and 3' SalI restriction sites. After amplification of the Strep-CNOT6L cDNA using oligonucleotides 5'-AAAAACCATGGCTAGCTGGAGCCAC-3' and 5'- GTTCTGAGGTCATTAAGTGG-3', the Strep-CNOT6L cDNA was inserted into the NcoI and SalI sites of multiple cloning site 1 of pACYC-Duet1 (Merck) containing a BamHI/SalI CNOT7 cDNA fragment inserted in the BglII/XhoI sites of multiple cloning site 2. After transformation of *E. coli* strain BL21 (DE3) with plasmids pQE80L-BTG2 and pACYCDuet-1/Strep-CNOT6L/CNOT7, protein expression (1 L LB medium) was induced at OD₆₀₀ 0.7-0.8 by the addition of isopropyl β-D-1-thiogalactopyranoside (IPTG; 0.2 mM final concentration) for 16 h at 18°C. Cell pellets were resuspended in 0.003 vol buffer SA (20 mM Tris-HCl pH 7.8, 250 mM NaCl, 10% glycerol, 2 mM β-mercaptoethanol), lysed by sonication (five cycles; 30 sec on/30 sec off; 60% amplitude, Qsonica XL2000),

and cleared by centrifugation (16,000×g for 45 min at 4°C). The soluble fraction was applied onto a 1 ml Strep-Tactin sepharose gravity column (IBA Life Sciences) and eluted with buffer SB (20 mM Tris-HCl pH 7.8, 250 mM NaCl, 10% glycerol, 1 mM β-mercaptoethanol, 10 mM D-Desthiobiotin) to isolate trimeric His•BTG2-Caf1-Strep•Ccr4 complexes. After collection of peak fractions, proteins were further purified by size-exclusion chromatography using a HiPrep 16/60 Sephacryl S-200 HR column (GE Healthcare) equilibrated and eluted in buffer GF (50 mM Tris-HCl pH 7.9, 250 mM NaCl, 5% glycerol, 1 mM β-mercaptoethanol). Peak fractions were pooled and concentrated using a Vivaspin concentrator (Sartorius). The inactive version containing amino acid substitutions D40A of Caf1 and E240A of Ccr4 was expressed and purified using the same procedure. Protein concentrations were determined using the Protein Assay Reagent (Bio-Rad) and purified proteins were stored in small aliquots at -80°C.

Expression and purification of the pentameric central module

To isolate the pentameric central module composed of BTG2-Caf1-Ccr4-CNOT1-CNOT9, the trimeric nuclease and CNOT1-CNOT9 modules were first expressed in *E. coli* BL21 (DE3) and purified separately.

The nuclease module was expressed and purified as described above. The CNOT1-CNOT9 dimer was obtained by co-expression of both proteins using plasmid pACYC-Duet1-CNOT1/CNOT9. This plasmid contained a codon-optimised cDNA encoding the MIF4G and DUF3819 domains of CNOT1 (amino acids 1093-1595) in multiple cloning site 1 and a human cDNA encoding the CNOT9 (ARM domain; amino acids 33-283) in multiple cloning site 2. Both cDNA fragments contained a 5' BamHI and a 3' SalI site, and were inserted into the corresponding sites of multiple cloning site 1 (CNOT1) or the 5' BglII and 3' XhoI sites of multiple cloning site 2 (CNOT9).

To purify the CNOT1-CNOT9 dimer, cells (1 L LB medium) were grown to OD₆₀₀ 0.7-0.8. After addition of IPTG (final concentration 0.2 mM), cultures were incubated for 16 h at 18°C and cells were harvested by centrifugation. The cell pellet was resuspended in 5 mL buffer HA (20 mM Tris-HCl pH 7.9, 250 mM NaCl, 1 mM β-mercaptoethanol, 5% glycerol and 20 mM imidazole) per litre of culture, lysed by sonication and the soluble lysate was isolated by centrifugation. The soluble lysate was then loaded onto a HisTrap FF pre-packed column (GE) equilibrated with buffer HA (20 mM Tris-HCl pH 7.9, 250 mM NaCl, 1 mM β-mercaptoethanol, 5% glycerol and 20 mM imidazole). After washing the unbound fraction, bound proteins were eluted using buffer HB (as buffer HA, but containing 250 mM imidazole) in 1 mL fractions.

The purified nuclease and CNOT1-CNOT9 dimer were then combined (molar ratio nuclease module:CNOT1-CNOT9 dimer = 1:1.2) and incubated for 16 h at 4°C to allow binding. Then, buffer was exchanged using a PD-10 column (GE) to buffer SA to remove D-desthiobiotin. After buffer exchange, the sample was loaded on a Poly-Prep gravity-flow column (Bio-Rad) packed with Strep-Tactin sepharose (IBA) and equilibrated with buffer SA (20 mM Tris-HCl pH 7.9, 250 mM NaCl, 1 mM β-mercaptoethanol and 5% glycerol). After washing the unbound fraction, the column was eluted using buffer SB. After exchanging the buffer composition to buffer SA using PD-10 columns (GE Healthcare), protein concentrations were determined using the Protein Assay Reagent (Bio-Rad). If necessary, protein samples were concentrated using Vivaspin spin columns (Sartorius). Purified proteins were flash-frozen and stored in small aliquots at -80°C.

Expression and purification of PABPC1

Full length His-PABPC1 and His-PABPC1 (1-190) were expressed and purified from *E. coli* BL21 (DE3) using plasmids pQE80L-PABPC1 and pQE80L-PABPC1 (1-190). Plasmid

pQE80L-PABPC1 for the expression of PABPC1 with an N-terminal hexahistidine tag was generated by reverse-transcriptase PCR of a full length cDNA using total RNA from HEK293 cells as a template. 5' BamHI and 3' SalI restriction sites were added, which facilitated cloning of the PCR product into the corresponding restriction sites of plasmid pQE80L (Qiagen). Plasmid pQE80L-PABPC1 (1-190) was generated using inverse PCR and subsequent ligation of the linear product.

After transformation of *E. coli* BL21 (DE3) with plasmid pQE80L-PABPC1 or pQE80L-PABPC1(1-190), cells were grown in 1 L LB medium at 37°C until the OD₆₀₀ was between 0.7-0.8. After addition of IPTG (final concentration of 0.2 mM), cultures were incubated for 16h at 18°C and cells were harvested by centrifugation. The cell pellet was resuspended in 5 mL buffer HA and lysed by sonication. The soluble lysate was isolated by centrifugation and then loaded on a HisTrap FF pre-packed column (GE) equilibrated with buffer HA. After washing the unbound fraction, proteins were eluted (1 mL fractions) using buffer HB. Peak fractions were pooled and concentrated using a Vivaspin column (Sartorius) and further purified by size-exclusion chromatography (HiPrep 16/60 Sephacryl S-200 HR, GE Healthcare) using buffer GF and collecting 2 mL fractions. Peak fractions were pooled and concentrated as described above. Protein concentrations were determined using the Protein Assay Reagent (Bio-Rad). Purified proteins were stored in small aliquots at -80°C and confirmed to be free of ribonuclease activity.

Enzyme assays

For quantitative fluorescence-based assays using short poly(A) tails, reactions (50 µl) were essentially carried out as described before [29]. Briefly, reactions contained 0.2 µM enzyme, 1.0 µM substrate (Fic-CCUUUCCAAAAA, Eurogentec), 20 mM Tris-HCl pH 7.9, 50 mM NaCl, 2 mM MgCl₂, 10% glycerol, 1 mM β-mercaptoethanol. After incubation at 30°C for the indicated times, aliquots (5 µl) were taken and reactions were stopped by addition of an equal volume of DNA probe mix (1.0% SDS, 3 µM DNA probe, TAMRA-TTTTTTTTTGGAAAGG, Eurogentec). After an overnight incubation in the dark, the fluorescence was measured using a Biotek Synergy HT plate reader. Fluorescence was measured at 25°C using the 485±20 nm and 528±20 nm filters for excitation and emission, respectively.

For gel-based assays using (A)₂₀ or (A)₅₀ RNA substrates, standard reactions (25 µl) contained 100 nM enzyme, 20 mM Tris-HCl pH 7.9, 50 mM NaCl, 2 mM MgCl₂, 10% glycerol, 1 mM β-mercaptoethanol and 0.2 µM 5'-Fic-labelled RNA substrate (Sigma-Genosys) in nuclease-free water. Reactions were incubated at 30°C and aliquots (3.5 µl) were taken at the following time points: 0, 5, 10, 20, 30, 40 and 60 min. RNA loading buffer (1.0 µl) was added and samples heated for 3-5 min at 85°C.

Reaction products were analysed by denaturing 20% polyacrylamide gel electrophoresis. Gels (acrylamide:bisacrylamide=19:1/50% urea, 1× TBE) were pre-run in 1× TBE at 300 V for 30 min before loading samples (3.0 µl). After running the gels (20-25 min at 300 V), reaction products were visualised by epi-fluorescence using a Fujifilm LAS-4000 instrument equipped with an epi-blue illuminator. Gel images were analysed using ImageJ (<https://imagej.nih.gov/ij/>) using the Multiplot/ROI Manager function and densitometry plots were prepared using GraphPad Prism.

To prepare PABPC1-poly(A) substrates, full length PABPC1 and a PABPC1 fragment encompassing RRM1 and RRM2 (amino acids 1-190) were used. PABPC1-poly(A)₂₀ substrates were prepared by incubating a 6-fold excess of full length PABPC1 or an 8-fold excess of PABPC1 RRM1-RRM2 (amino acids 1-190) with poly(A)₂₀ RNA for 15 min

at room temperature (20 mM Tris-HCl pH 7.9, 50 mM NaCl, 2 mM MgCl₂, 10% glycerol, 1 mM β-mercaptoethanol and 0.2 μM 5'-Flc-labelled poly(A)₂₀ RNA substrate in nuclease-free water) prior to the addition of enzyme.

Computational analysis of protein structure

To model the P131L amino acid substitution of CNOT9, the structure of a CNOT1-CNOT9 complex (PDB accession number 4CRV) was used [15]. Pro-131 was substituted with five leucine rotamers with the highest probabilities (accumulated probability 0.994) according to the Dunbrack rotamer library and clashes and contacts with neighbouring atoms were then identified [30]. Subsequently, the structure was minimised to accommodate the substituted rotamer. The UCSF Chimera package was used for structure visualisation and analysis [31]. For energy minimisation, Molecular Modeling Toolkit routines and Amber parameters were used [32, 33].

Differential scanning fluorimetry

Plasmid pQE80L-TEV-CNOT9 was made by inserting a codon-optimised CNOT9 cDNA (amino acids 33-283; using a 5' BamHI and a 3' SalI restriction site) into a modified pQE80L vector containing a TEV protease site following the N-terminal His-tag. The P131L variant of CNOT9 was generated by site-directed mutagenesis using a modified Quikchange protocol (Agilent). Proteins were expressed in *E. coli* BL21 (DE3) and purified using immobilised metal-affinity chromatography as described above. Differential scanning fluorimetry (thermal stability assay) was carried out using an Agilent MX3005p instrument and the fluorescent dye SYPRO Orange (5000× in DMSO, ThermoFisher Scientific) [34]. Standard assays (20 μl) contained: 2.5-10 μM purified CNOT9 or the P131L variant, 20 mM Tris-HCl pH 7.8, 500 mM NaCl, 10% glycerol, 1 mM β-mercaptoethanol, 5x SYPRO Orange dye. Reactions were performed in PCR-grade 96-well thin-wall plates. After sealing with optical-grade lids, reactions were collected at the bottom of the wells by centrifugation. Fluorescence scanning was carried out using a temperature gradient from 25°C to 95°C at 1°C per minute using the FAM (492 nm) filter for excitation and the ROX (610 nm) filter for detection. Each experiment contained three technical replicates. Data was acquired using MxPro QPCR software (Agilent), and analysed using Microsoft Excel 2013 and Graphpad Prism (version 7) as described [34].

Results

Reconstitution of the central module of the human Ccr4-Not complex

To understand the biochemical mechanism of deadenylation by the human Ccr4-Not complex, we recently reported the reconstitution of a trimeric nuclease module composed of human BTG2-Caf1-Ccr4 [27]. To begin to investigate the contribution of the non-catalytic subunits of Ccr4-Not, we aimed to expand the nuclease module by including the central region of CNOT1 encompassing the MIF4G and DUF3819 domains (also known as the middle region CNOT1M [15]) and the CNOT9 subunit (Figure 1A, 1B). To this end, we explored various strategies. Co-expression of all five proteins in *Escherichia coli* resulted in a mixture of sub-complexes that were difficult to separate and relatively poor yields. Instead, separate expression and purification of the nuclease module and a CNOT1M-CNOT9 dimer, followed by reconstitution of the pentameric complex resulted in a robust procedure (Figure 1C). Thus, the components of the nuclease module, BTG2, Caf1 and Ccr4, were co-expressed as described before [27] except for the use of Ccr4 tagged with a Twin-Step tag (Figure 1D). In parallel, the CNOT1M-CNOT9 dimer was obtained by co-expression of His-tagged CNOT1 (amino

acids 1093-1595) and CNOT9 (amino acids 33-285) in bacterial cells followed by purification of the dimeric complex using immobilised metal-affinity chromatography (Figure 1D). The pentameric BTG2-Caf1-Ccr4-CNOT1-CNOT9 complex was then reconstituted by mixing the CNOT1M-CNOT9 dimer and the trimeric BTG2-Caf1-Ccr4 nuclease module, following by a second round of Strep-affinity purification (Figure 1D). We termed this complex the central module reflecting the fact that this complex represents the proteins bound to the central region of CNOT1 encompassing the MIF4G and DUF3819 domains.

CNOT1 (MIF4G-DUF3819) and CNOT9 stimulate deadenylation by the nuclease module

As a first step to evaluate the contribution of the CNOT1 central region and the CNOT9 subunit on the activity of the nuclease module, the activity of the complex was determined using a quantitative fluorescence-based assay [29]. In parallel, deadenylation by the nuclease module, Caf1 and the Caf1-BTG2 dimer was also determined. Analysis by SDS-PAGE showed that the protein samples contained similar amounts of the Caf1 subunit (Figure 2A). We then measured the activities of equimolar amounts of Caf1 and Caf1-containing complexes using a synthetic 16-mer oligonucleotide containing nine terminal adenosine residues as a substrate. In these assays, it was apparent that the activity of the central module was consistently higher than that of the nuclease module indicating that the CNOT1 central domain and CNOT9 stimulate the activity of the nuclease module. Moreover, we confirmed our previous observations that the nuclease module has increased activity as compared to the BTG2-Caf1 dimer, which in turn displays greater deadenylation compared to the isolated Caf1 protein [27]. No activity was detected when catalytically inactive protein preparations were used, indicating that the observed activities were due to the catalytic activities of the purified proteins (Figure 2B).

BTG2 stimulates the nuclease activity of Caf1

Next, we assessed deadenylation in more detail using a 5' fluorescein-labelled synthetic oligonucleotide containing 20 adenosine residues (Flc-A₂₀) followed by product analysis using denaturing gel electrophoresis. Under conditions where the activity of Caf1 was barely measurable (Figure 3A), activity of the BTG2-Caf1 dimer was clearly detected (Figure 3B). This indicates that BTG2 stimulates the deadenylation activity of Caf1 ($p < 0.05$, Supplementary Figure S1) in agreement with our previous observation that BTG2 stimulates the ribonuclease activity of Caf1 [27].

Next, we investigated degradation of poly(A) in the presence of cytoplasmic poly(A)-binding protein PABPC1. We used a six-fold molar excess (protein:RNA) that resulted in binding of the majority of the poly(A) oligonucleotide substrate by PABPC1 (Supplementary Figure S2). While the presence of PABPC1 did not affect the activity of Caf1 (compare Figure 3C and 3A), degradation of poly(A) by the BTG2-Caf1 dimer was increased in the presence of PABPC1 (compare Figure 3D and 3B; $p < 0.05$, Supplementary Figure S1). This is in agreement with recent findings reported by Stupfler *et al* [35].

We then assessed deadenylation in the presence of a fragment of PABPC1 containing RRM1 and RRM2 (amino acid residues 1-190). Using an eight-fold molar excess (protein:RNA), virtually all poly(A) molecules were bound by one molecule of the PABPC1 RRM1-RRM2 fragment as determined by a gel-shift assay (Supplementary Figure S2). As expected [35], these results mimicked those obtained with full length PABPC1: the presence of PABPC1 RRM1-RRM2 did not affect the activity of Caf1 (compare Figure 3E

and 3A), whereas deadenylation by BTG2-Caf1 was increased in the presence of the PABPC1 RRM1-RRM2 fragment (compare Figure 3F and 3B; $p < 0.05$, Supplementary Figure S1). The activity of BTG2-Caf1 was stimulated by the PABPC1 RRM1-RRM2 fragment to a similar extent as full length PABPC1 (compare Figure 3F and 3E, Supplementary Figure S1). Similar results were observed when a substrate containing 50 adenosine residues was used (Supplementary Figure S3-S5).

Deadenylation by the nuclease and central modules in the presence of poly(A)-binding protein PABPC1

When assessing deadenylation using a 5' fluorescein-labelled synthetic oligonucleotide containing 20 adenosine residues (Flc-A₂₀), the nuclease module displayed robust activity with fully deadenylated products detectable at later time points (Figure 4A). Compared to the nuclease module, faster deadenylation was observed in the presence of equimolar concentrations of the central module, with fully deadenylated products detected as the major product after 30 minutes (Figure 4B). These results confirm that the activity of the nuclease module is stimulated by the central module of CNOT1 and the CNOT9 subunit ($p < 0.05$; Supplementary Figure S1).

In the presence of PABPC1, stimulation of the activities of the nuclease and central modules was less evident. At earlier time points (5-20 min), deadenylation by the nuclease and central modules was further increased (Figure 4C, 4D). However, at later time points, a transient accumulation of partially deadenylated products was observed in the presence of PABPC1, which was not noticeable in the absence of PABPC1. This observation suggests a pause, which was observed after removal of approximately 12 adenosine residues. A similar pattern of deadenylation was observed in the presence of a PABPC1 fragment encompassing RRM1 and RRM2 (Figure 4E and 4F) or when a substrate containing a 50 adenosine tail was used (Supplementary Figure S2-S4). When using this longer substrate, which can accommodate two molecules of PABPC1, two intermediate products were observed.

Together, these results confirm that the central region of CNOT1 and the CNOT9 subunit contribute to the activity of the Ccr4-Not complex by stimulating the enzymatic activity of the nuclease module. In addition, these results indicate that PABPC1 can pose a transient block, which does not appear to involve the third and fourth RRM and the C-terminal domain of PABPC1, because intermediary products are also observed in the presence of a PABPC1 fragment composed of RRM1 and RRM2.

The thermal stability of CNOT9 is reduced by the lymphoma-associated P131L amino acid substitution

Having established a positive role for the central fragment of CNOT1 and the CNOT9 subunit in deadenylation, we investigated the impact of the amino acid substitution P131L of CNOT9. This amino acid alteration is frequently observed in melanoma tumours due to a recurrent somatic T→C mutation. Residue Pro-131 is located in α -helix 8 and in close proximity to α -helix 5 (Figure 5A). Based on its location, substitution P131L is unlikely to directly disrupt interactions with the DUF3819 domain of CNOT1, or interactions mediated by the tryptophan-binding pockets of CNOT9, which are involved in interactions with GW182 and TTP [11, 15] (Figure 5A). However, computational analysis of the P131L amino acid substitution indicates multiple clashes with several backbone and side-chain atoms of residues Leu-82, Thr-83, Ala-84 and Ser-87 located in α -helix 5 (Figure 5B). As a consequence, it is likely that structural changes are required to accommodate the P131L alteration.

Therefore, we tested the thermal stability of CNOT9 and the CNOT9 P131L variant by differential scanning fluorimetry (DSF). To this end, purified CNOT9 proteins were subjected to a temperature gradient and thermal stability (represented by the melting temperature T_m) of CNOT9 was determined by real-time measurement of fluorescence in the presence of the dye SYPRO Orange, which represents protein unfolding (Figure 5C). The experiments indicated that CNOT9 P131L showed a reduced T_m ($\Delta T_m = -2.60 \pm 0.04^\circ\text{C}$) (Figure 5C and 5D) consistent with decreased stability of CNOT9 due to structural rearrangements to accommodate the P131L amino acid alteration.

The central module containing the melanoma-associated CNOT9 P131L variant supports deadenylation

To test whether the reduced thermal stability of the P131L variant of CNOT9 affects the activity of the central module, we purified the central module containing the variant CNOT9 subunit. Expression and purification of the CNOT1-CNOT9 P131L complex in bacterial cells resulted in similar yields and purity compared to the wild type complex. In addition, reconstituted central modules containing CNOT9 P131L were readily obtained (Figure 6A). To test whether the P131L amino acid substitution of CNOT9 impacts on deadenylation by the central module, we evaluated the activity of equimolar amounts of the module containing wild type or P131L CNOT9. Comparison of the deadenylase activities of the complexes shows that the central module containing the CNOT9 P131L subunit displayed robust nuclease activity that is comparable to that of the wild type module (Figure 6B and 6C; Supplementary Figure S1).

Together, these results indicate that the recurrent melanoma-associated amino acid substitution P131L does affect the thermal stability of CNOT9, but does not significantly impact on the deadenylation activity of the central module.

Discussion

The main findings reported here are: (i) we describe a procedure to reconstitute a pentameric sub-complex of Ccr4-Not, termed the central module, which is composed of the central region of CNOT1 containing the MIF4G and DUF3819 domains, the CNOT9 subunit, and a trimeric nuclease module composed of BTG2, Caf1 and Ccr4; (ii) the pentameric central module of Ccr4-Not has a higher deadenylation activity as compared to the trimeric nuclease module revealing a new role for the central region of CNOT1 and CNOT9; and (iii) the melanoma-associated CNOT9 P131L variant supports deadenylation similar to the wild type subunit in the context of the pentameric central module of Ccr4-Not. In addition, we also show that BTG2 stimulates the activity of Caf1, which is further enhanced in the presence of cytoplasmic poly(A)-binding protein PABPC1 in agreement with results reported by Stupfler *et al.* [35].

The role of the non-catalytic subunits

The non-catalytic subunits of the Ccr4-Not complex are known to mediate interactions with RNA-binding factors that regulate RNA stability. In this regard, protein-protein interactions involving regulatory proteins and the CNOT1 and CNOT9 subunits are particularly well characterised. For example, the developmental regulator Nanos interacts with CNOT1 [8, 9], whereas *Drosophila* Bag-of-marbles and Roquin interact with the CNOT9 subunit [13, 36]. Moreover, GW182, a component of the miRNA-repression complex, and the A/U-rich element binding protein TTP interact with both the CNOT1 and CNOT9 proteins [11-13, 15, 16, 36]. Interestingly, all known interactions

between regulatory factors and CNOT1 involve sequences outside the central region of CNOT1 studied here.

A role for the non-catalytic subunits involved in stimulating the activity of the nuclease module was described for the *S. pombe* complex [26]. In this case, the reconstituted complex composed of eight subunits displays a significantly higher activity than the isolated nuclease module. Our findings presented here demonstrate that the central region of CNOT1 encompassing the MIF4G and DUF3819 domains together with CNOT9 increase the activity of the human nuclease module. There are at least two possible mechanisms by which the complex of CNOT1 and CNOT9 may enhance the activity of the nuclease module. Firstly, the non-catalytic subunits may regulate the activity of the nuclease subunits via an allosteric mechanism and induce a conformation with higher activity. Alternatively, the non-catalytic subunits may interact with RNA, thereby enhancing the affinity for the substrate. Although CNOT9 can interact with nucleic acids [37], it is not obvious from the available structural information how this would lead to increased degradation of the poly(A) substrate used. Further structural information integrating available information of isolated modules is required to provide a rationale for the experimental observations presented here.

The melanoma-associated CNOT9 P131L variant

Exome sequencing of metastatic melanoma samples led to the identification of a variant CNOT9 subunit containing the P131L amino acid substitution [28]. This variant is found in a subset of melanoma cell lines and tumours and is caused by a T→C transition induced by exposure to UV light. Typically, this mutation only affects one allele suggesting that both the P131L variant and the wild type protein are present in melanoma cells. Modelling the P131L amino acid change suggests that the substitution is unlikely to directly affect the tryptophan-binding pockets of CNOT9, which are involved in interactions with GW182 and TTP [11, 15, 16]. Moreover, while the amino acid change affects the structural stability of CNOT9 as determined by differential scanning fluorimetry, the central module containing the CNOT9 P131L subunit is able to support deadenylation comparable to the central module containing wild type CNOT9. Based on this observation, we propose that the P131L amino acid change may affect specific protein-protein interactions involving CNOT9, or result in reduced protein levels due to decreased cellular stability.

Deadenylation in the presence of PABPC1

BTG2 is a member of a small protein family that includes BTG1-4, TOB1 and TOB2 [38, 39], which stimulate deadenylation and mRNA degradation [40-43]. Recently, it was demonstrated that BTG2 can enhance deadenylation by the isolated Caf1 protein in the presence of PABPC1 [35]. Although our results indicate that BTG2 can also increase the activity of Caf1 in the absence of PABPC1, a further stimulation of Caf1 activity is observed in the presence of PABPC1 or a fragment of PABPC1 containing the RRM1 and RRM2 domains in agreement with results previously reported by Stupfler *et al* [35]. However, stimulation of deadenylation by PABPC1 was less evident in the presence of the nuclease and central modules, which display a much increased activity as compared to the dimeric complex composed of BTG2 and Caf1. While degradation of poly(A) containing 20 residues by the nuclease and central modules was increased at early time points in the presence of PABPC1 or the fragment containing the first two RRM domains, a transient accumulation of intermediary products was observed at later time points. Interestingly, the length of the transiently accumulated product is about eight nucleotides, which corresponds to the number of nucleotides that interact with RRM1 and

RRM2 of PABPC1 [44]. This suggests that dissociation of PABPC1 is required for complete degradation of the substrate. When longer substrates were used that can accommodate the binding of two PABPC1 molecules, an additional intermediary product was observed (Supplementary Figure S3-S4).

In summary, the work presented here reveals a role for central region of CNOT1 and the non-catalytic CNOT9 subunit in stimulating the activity of the nuclease module of the Ccr4-Not complex. Moreover, it demonstrated that the melanoma-associated CNOT9 P131L variant retains the ability to be incorporated into the central module of the complex and supports enhanced deadenylation of the mutant central module.

Acknowledgements

This work was supported by a University of Nottingham Vice-Chancellor's Scholarship for Research Excellence (L.P.), the Biotechnology and Biological Sciences Research Council (BBSRC) Doctoral Training Programme at the University of Nottingham (B.H.), and a Faculty for the Future scholarship of the Schlumberger Foundation (B.A.). Emma Gunnell and Ingrid Dreveny are gratefully acknowledged for helpful discussions.

Declarations of interest

None

Author contributions

The study was conceived by G.S.W. The experiments were designed by L.P. and G.S.W. L.P. carried out all experiments shown in Figures 1-6 and the supplementary material. B.H. constructed the pQE80L expression vector containing a TEV protease site and prepared several CNOT9 and CNOT9 P131L constructs for prokaryotic expression. B.A. modified the procedure for purification of the trimeric nuclease module using co-expression of Strep-tagged Ccr4/CNOT6L, Caf1/CNOT7 and His-BTG2. Data was analysed by L.P. and G.S.W. The manuscript was prepared by L.P. and G.S.W. All authors read and approved the final manuscript.

Figures

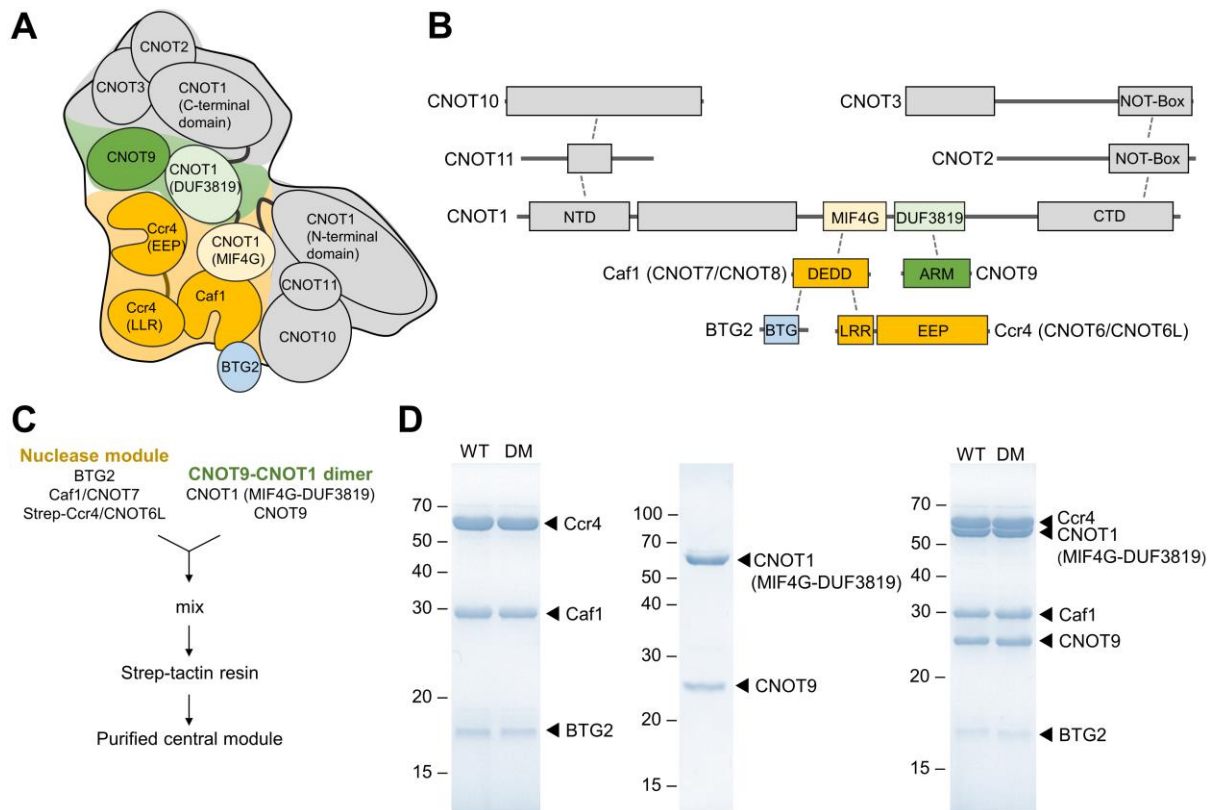


Figure 1. Reconstitution of a Ccr4-Not central module composed of BTG2-Caf1-Ccr4-CNOT1^{MIF4G-DUF3869}-CNOT9. (A) Schematic diagram of the Ccr4-Not complex. Highlighted are the nuclease module (yellow), the BTG2 protein (blue) and the CNOT9 module (green). The location of the subunits is based on the structure of the *Saccharomyces cerevisiae* Ccr4-Not complex [45]. (B) Diagram of the subunit organisation in the Ccr4-Not complex. Indicated are known domains involved in protein-protein interactions between subunits. The central region of CNOT1 (amino acids 1093-1595) encompasses the MIF4G and DUF3819 domains. (C) Overview of the purification strategy. (D) Purification of the nuclease module (*left panel*), the CNOT1-CNOT9 dimer (*middle*) and the reconstituted central module composed of BTG2, Caf1/CNOT7, Ccr4/CNOT6L, CNOT1 (MIF4G-DUF3869) and CNOT9 (*right*). Purified protein complexes (5 μ g) were subjected to 14% SDS-PAGE and stained with Coomassie.

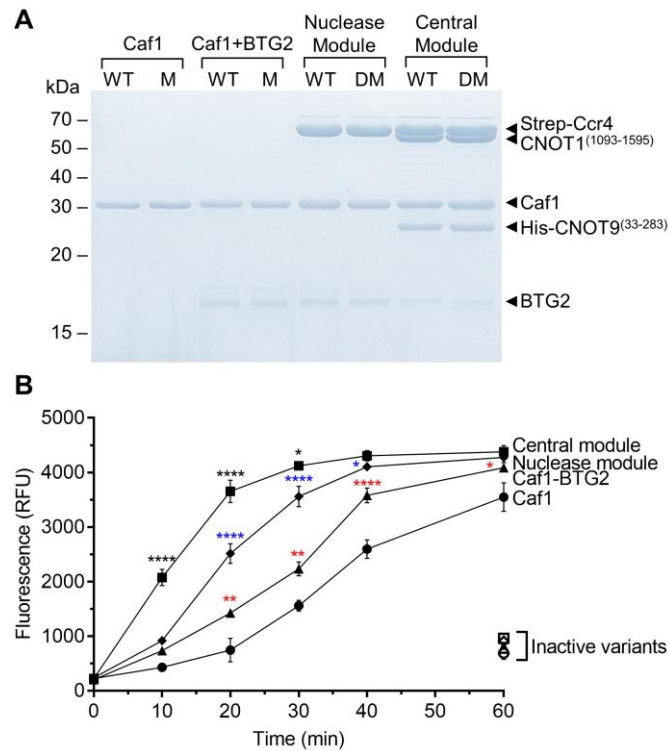


Figure 2. Deadenylation by the nuclease module is stimulated by the central region of CNOT1 and CNOT9. (A) Analysis of Caf1 and Caf1-containing complexes. Proteins were separated by 14% SDS-PAGE and visualised by Coomassie staining. M, Caf1 D40A mutant; DM (double mutant), complexes containing inactive nuclease subunits Caf1 D40A/Ccr4 E240A. (B) Deadenylation by Caf1, the Caf1-BTG2 dimer, the nuclease module composed of BTG2, Caf1 and Ccr4, and the central module composed of BTG2, Caf1, Ccr4, the central region of CNOT1 and CNOT9. Reactions contained a synthetic 16-mer oligonucleotide with nine terminal adenosine residues (1.0 μ M) which were incubated with the indicated enzymes (200 nM) at 30°C for the indicated time. Deadenylation was determined by measuring fluorescence as described previously [29]. Error bars indicate the standard error of the mean (n=4). * P<0.05; ** P<0.01, **** P<0.0001; black, nuclease compared to central module; blue, nuclease complex compared to Caf1-BTG2 complex; red, Caf1-BTG2 complex compared to Caf1. P values were calculated using a two-way ANOVA/Tukey test using Graphpad Prism 7.04.

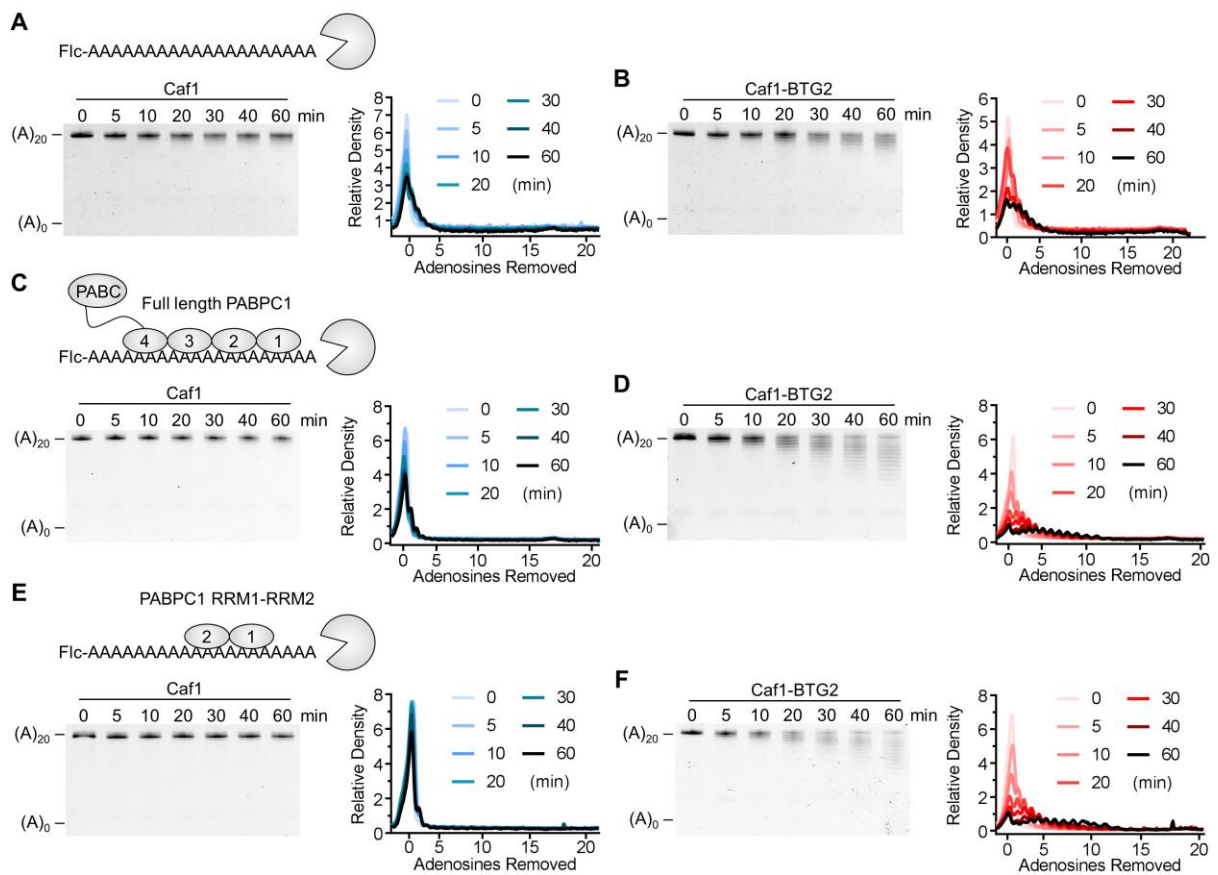


Figure 3. BTG2 stimulates the activity of Caf1. (A) Deadenylation of poly(A) by Caf1. (B) Deadenylation of poly(A) by the Caf1-BTG2 dimer. (C) Deadenylation of poly(A) in the presence of full length PABPC1 by Caf1. (D) Deadenylation of poly(A) in the presence of full length PABPC1 by the BTG2-Caf1 dimer. (E) Deadenylation of poly(A) in the presence of PABPC1 RRM1-RRM2 by Caf1. (F) Deadenylation of poly(A) in the presence of PABPC1 RRM1-RRM2 by the BTG2-Caf1 dimer. Synthetic oligonucleotides (200 nM 5'Fic-(A)₂₀) were incubated with the indicated enzymes (100 nM) at 30°C and stopped at the indicated time points. Products were analysed by denaturing 50% urea/20% PAGE (*left*). Densitometric analysis was carried out using ImageJ (*right*).

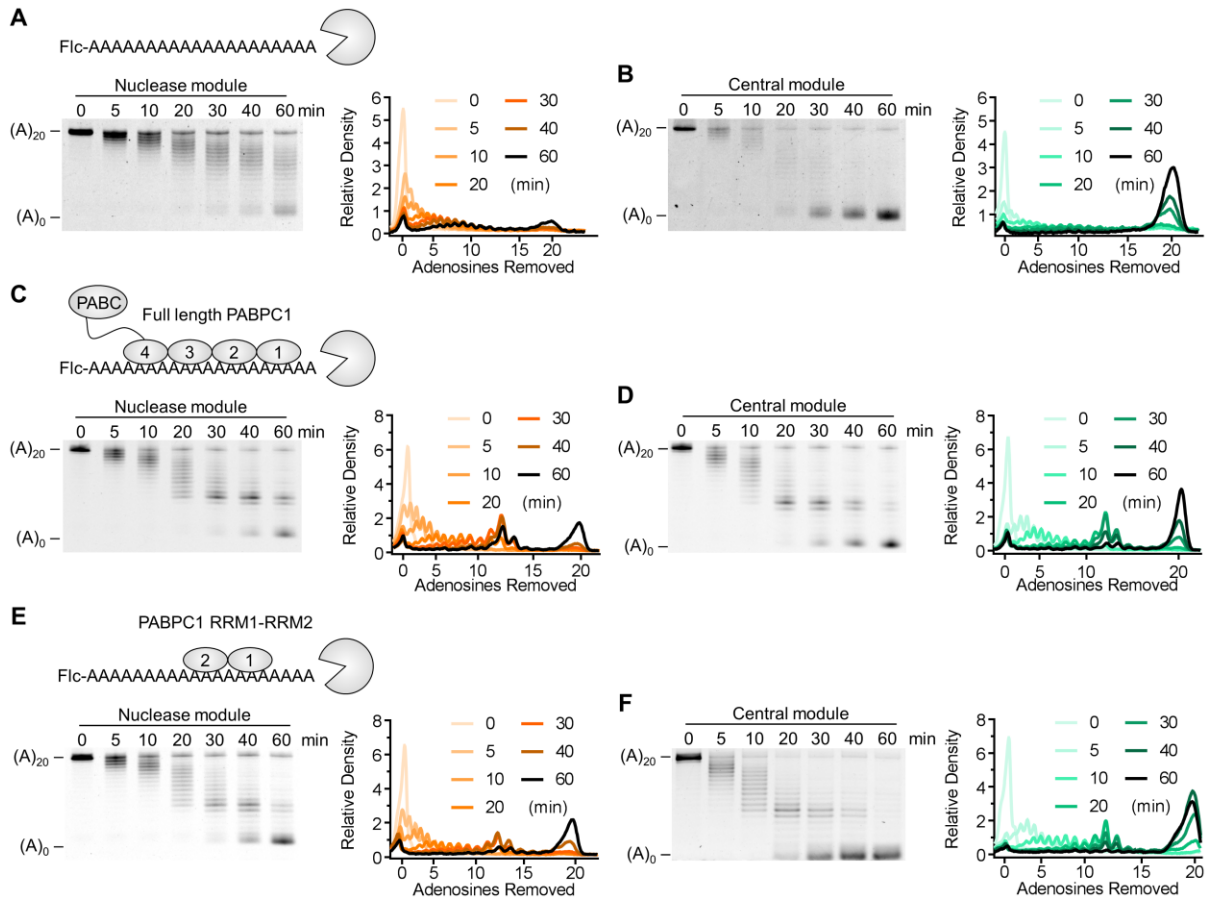


Figure 4. The central region of CNOT1 and CNOT9 enhance the activity of the nuclease module. (A) Deadenylation of poly(A) by the trimeric nuclease module. (B) Deadenylation of poly(A) by the pentameric central module. (C) Deadenylation of poly(A) in the presence of full length PABPC1 by the trimeric nuclease module. (D) Deadenylation of poly(A) in the presence of full length PABPC1 by the pentameric central module. (E) Deadenylation of poly(A) in the presence of PABPC1 RRM1-RRM2 by the trimeric nuclease module. (F) Deadenylation of poly(A) in the presence of PABPC1 RRM1-RRM2 by the pentameric central module. Synthetic oligonucleotides (200 nM 5'Flc-(A)₂₀) were incubated with the indicated enzymes (100 nM) at 30°C and stopped at the indicated time points. Products were analysed by denaturing 50% urea/20% PAGE (*left*). Densitometric analysis was carried out using ImageJ (*right*).

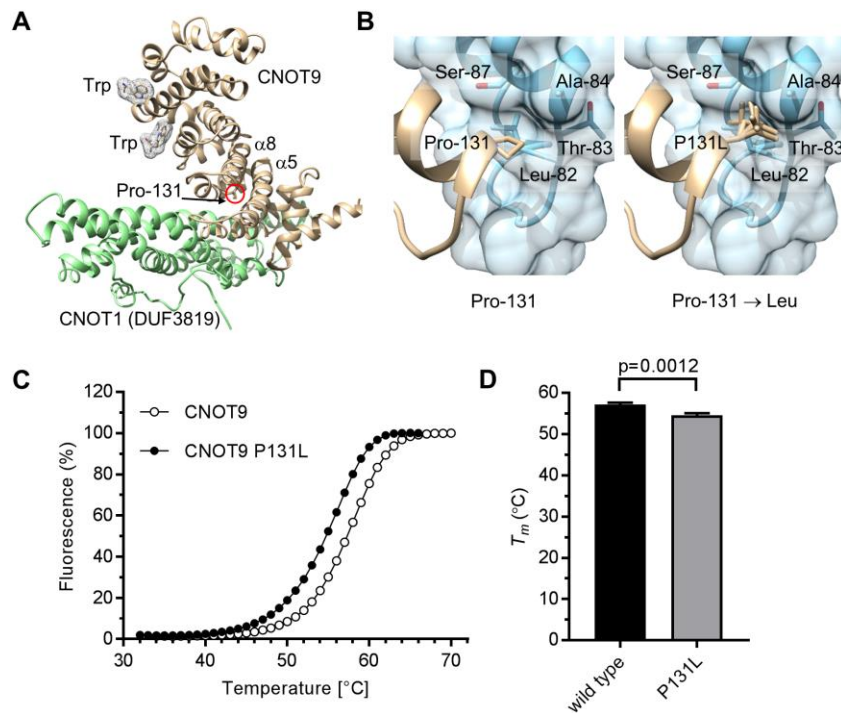


Figure 5. Reduced thermal stability caused by the CNOT9 P131L amino acid substitution. (A) Overview of the CNOT9-CNOT1 (DUF3819) protein complex (PDB 4CRV) [15]. Indicated are CNOT9 (tan), the DUF3819 domain of CNOT1 (green), the position of Pro-131 of CNOT9 (part of α -helix $\alpha 8$), the neighbouring α -helix $\alpha 5$, and the two tryptophan binding pockets of CNOT9. (B) The Pro-131 \rightarrow Leu amino acid substitution is predicted to result in multiple clashes with α -helix $\alpha 5$. Indicated are α -helix $\alpha 8$ (tan), including the position of Pro-131 (left) and the modelling of leucine rotamers (right), α -helix $\alpha 5$ (blue), including amino acids that display multiple predicted clashes with leucine rotamers. (C) Differential scanning fluorimetry of CNOT9 and CNOT9 P131L. Wild type and CNOT9 P131L (5.0 μ M) was incubated in the presence of SYPRO Orange dye and subjected to a temperature gradient from 25 to 95°C (1 min/°C). (D) Reduced thermal stability of CNOT9 P131L (grey) compared to wild type CNOT9 (black). $\Delta T = -2.60 \pm 0.04^\circ\text{C}$ (mean \pm standard error; $n=8$). The p -value was calculated using a two-tailed t -test.

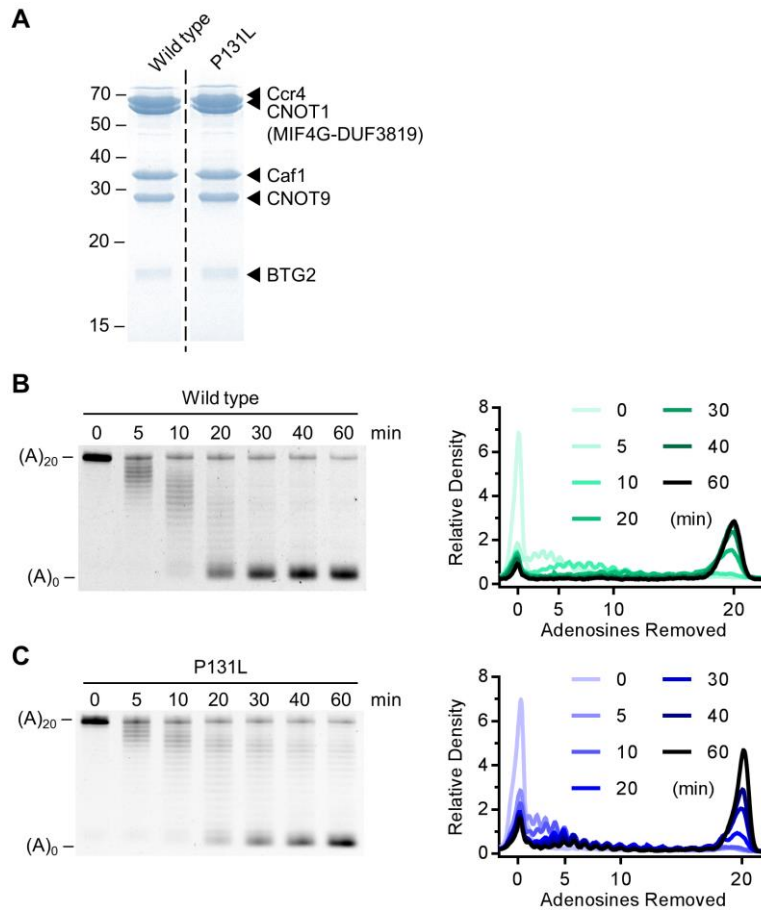


Figure 6. The central module containing the CNOT9 P131L variant supports deadenylation. (A) Purification of pentameric core complexes containing wild type CNOT9 and CNOT9 P131L. Purified protein complexes (5 μ g) were subjected to 14% SDS-PAGE and stained with Coomassie. (B) Deadenylation of poly(A) by the pentameric core complex containing wild type CNOT9. (C) Deadenylation of poly(A) by the pentameric core complex containing the melanoma-associated CNOT9 P131L variant. Substrate (200 nM 5'Flc-(A)₂₀) was incubated with the indicated enzymes (100 nM) at 30°C and stopped at the indicated time points. Products were analysed by denaturing 50% urea/20% PAGE (*left*). Densitometric analysis was carried out using ImageJ (*right*).

References

- 1 Chen, C. Y. and Shyu, A. B. (2011) Mechanisms of deadenylation-dependent decay. Wiley interdisciplinary reviews. RNA. **2**, 167-183
- 2 Garneau, N. L., Wilusz, J. and Wilusz, C. J. (2007) The highways and byways of mRNA decay. Nat Rev Mol Cell Biol. **8**, 113-126
- 3 Parker, R. and Song, H. (2004) The enzymes and control of eukaryotic mRNA turnover. Nature Struct. Mol. Biol. **11**, 121-127
- 4 Goldstrohm, A. C. and Wickens, M. (2008) Multifunctional deadenylase complexes diversify mRNA control. Nat Rev Mol Cell Biol. **9**, 337-344
- 5 Jonas, S. and Izaurralde, E. (2015) Towards a molecular understanding of microRNA-mediated gene silencing. Nat Rev Genet. **16**, 421-433
- 6 Wahle, E. and Winkler, G. S. (2013) RNA decay machines: Deadenylation by the Ccr4-Not and Pan2-Pan3 complexes. Biochim Biophys Acta. **1829**, 561-570
- 7 Goldstrohm, A. C., Seay, D. J., Hook, B. A. and Wickens, M. (2007) PUF protein-mediated deadenylation is catalyzed by Ccr4p. J. Biol. Chem. **282**, 109-114
- 8 Bhandari, D., Raisch, T., Weichenrieder, O., Jonas, S. and Izaurralde, E. (2014) Structural basis for the Nanos-mediated recruitment of the CCR4-NOT complex and translational repression. Genes & development. **28**, 888-901
- 9 Suzuki, A., Igarashi, K., Aisaki, K., Kanno, J. and Saga, Y. (2010) NANOS2 interacts with the CCR4-NOT deadenylation complex and leads to suppression of specific RNAs. Proc Natl Acad Sci U S A. **107**, 3594-3599
- 10 Sandler, H., Kreth, J., Timmers, H. T. and Stoecklin, G. (2011) Not1 mediates recruitment of the deadenylase Caf1 to mRNAs targeted for degradation by tristetraprolin. Nucleic Acids Res. **39**, 4373-4386
- 11 Bulbrook, D., Brazier, H., Mahajan, P., Kliszczak, M., Fedorov, O., Marchese, F. P., Aubareda, A., Chalk, R., Picaud, S., Strain-Damerell, C., Filippakopoulos, P., Gileadi, O., Clark, A. R., Yue, W. W., Burgess-Brown, N. A. and Dean, J. L. E. (2018) Tryptophan-Mediated Interactions between Tristetraprolin and the CNOT9 Subunit Are Required for CCR4-NOT Deadenylase Complex Recruitment. Journal of Molecular Biology. **430**, 722-736
- 12 Fabian, M. R., Frank, F., Rouya, C., Siddiqui, N., Lai, W. S., Karetnikov, A., Blackshear, P. J., Nagar, B. and Sonenberg, N. (2013) Structural basis for the recruitment of the human CCR4-NOT deadenylase complex by tristetraprolin. Nature structural & molecular biology. **20**, 735-739
- 13 Sgromo, A., Raisch, T., Bawankar, P., Bhandari, D., Chen, Y., Kuzuoglu-Ozturk, D., Weichenrieder, O. and Izaurralde, E. (2017) A CAF40-binding motif facilitates recruitment of the CCR4-NOT complex to mRNAs targeted by Drosophila Roquin. Nat Commun. **8**, 14307
- 14 Leppek, K., Schott, J., Reitter, S., Poetz, F., Hammond, M. C. and Stoecklin, G. (2013) Roquin Promotes Constitutive mRNA Decay via a Conserved Class of Stem-Loop Recognition Motifs. Cell. **153**, 869-881
- 15 Chen, Y., Boland, A., Kuzuoglu-Ozturk, D., Bawankar, P., Loh, B., Chang, C. T., Weichenrieder, O. and Izaurralde, E. (2014) A DDX6-CNOT1 complex and W-binding pockets in CNOT9 reveal direct links between miRNA target recognition and silencing. Mol Cell. **54**, 737-750
- 16 Mathys, H., Basquin, J., Ozgur, S., Czarnocki-Cieciura, M., Bonneau, F., Aartse, A., Dziembowski, A., Nowotny, M., Conti, E. and Filipowicz, W. (2014) Structural and biochemical insights to the role of the CCR4-NOT complex and DDX6 ATPase in microRNA repression. Mol Cell. **54**, 751-765
- 17 Xu, K., Bai, Y., Zhang, A., Zhang, Q. and Bartlam, M. G. (2014) Insights into the structure and architecture of the CCR4-NOT complex. Front Genet. **5**, 137
- 18 Bawankar, P., Loh, B., Wohlbold, L., Schmidt, S. and Izaurralde, E. (2013) NOT10 and C2orf29/NOT11 form a conserved module of the CCR4-NOT complex that docks onto the NOT1 N-terminal domain. RNA biology. **10**, 228-244
- 19 Mauxion, F., Preve, B. and Seraphin, B. (2013) C2ORF29/CNOT11 and CNOT10 form a new module of the CCR4-NOT complex. RNA biology. **10**, 267-276

- 20 Bhaskar, V., Roudko, V., Basquin, J., Sharma, K., Urlaub, H., Seraphin, B. and Conti, E. (2013) Structure and RNA-binding properties of the Not1-Not2-Not5 module of the yeast Ccr4-Not complex. *Nature structural & molecular biology*. **20**, 1281-1288
- 21 Boland, A., Chen, Y., Raisch, T., Jonas, S., Kuzuoglu-Ozturk, D., Wohlbold, L., Weichenrieder, O. and Izaurralde, E. (2013) Structure and assembly of the NOT module of the human CCR4-NOT complex. *Nature structural & molecular biology*. **20**, 1289-1297
- 22 Basquin, J., Roudko, V. V., Rode, M., Basquin, C., Seraphin, B. and Conti, E. (2012) Architecture of the nuclease module of the yeast Ccr4-not complex: the Not1-Caf1-Ccr4 interaction. *Mol Cell*. **48**, 207-218
- 23 Petit, A. P., Wohlbold, L., Bawankar, P., Huntzinger, E., Schmidt, S., Izaurralde, E. and Weichenrieder, O. (2012) The structural basis for the interaction between the CAF1 nuclease and the NOT1 scaffold of the human CCR4-NOT deadenylase complex. *Nucleic Acids Res*. **40**, 11058-11072
- 24 Viswanathan, P., Ohn, T., Chiang, Y. C., Chen, J. and Denis, C. L. (2004) Mouse CAF1 can function as a processive deadenylase/3'-5'-exonuclease in vitro but in yeast the deadenylase function of CAF1 is not required for mRNA poly(A) removal. *The Journal of biological chemistry*. **279**, 23988-23995
- 25 Niinuma, S., Fukaya, T. and Tomari, Y. (2016) CCR4 and CAF1 deadenylases have an intrinsic activity to remove the post-poly(A) sequence. *RNA*. **22**, 1550-1559
- 26 Stowell, J. A. W., Webster, M. W., Kogel, A., Wolf, J., Shelley, K. L. and Passmore, L. A. (2016) Reconstitution of Targeted Deadenylation by the Ccr4-Not Complex and the YTH Domain Protein Mmi1. *Cell Rep*. **17**, 1978-1989
- 27 Maryati, M., Airhihen, B. and Winkler, G. S. (2015) The enzyme activities of Caf1 and Ccr4 are both required for deadenylation by the human Ccr4-Not nuclease module. *Biochem J*. **469**, 169-176
- 28 Wong, S. Q., Behren, A., Mar, V. J., Woods, K., Li, J., Martin, C., Sheppard, K. E., Wolfe, R., Kelly, J., Cebon, J., Dobrovic, A. and McArthur, G. A. (2015) Whole exome sequencing identifies a recurrent RQCD1 P131L mutation in cutaneous melanoma. *Oncotarget*. **6**, 1115-1127
- 29 Maryati, M., Kaur, I., Gopal, J., Olotu-Umoren, L., Oveh, B., Hashmi, L., Fischer, P. M. and Winkler, G. S. (2014) A fluorescence-based assay suitable for quantitative analysis of deadenylase enzyme activity. *Nucleic Acids Res*. **42**, e30
- 30 Dunbrack, R. L., Jr. and Karplus, M. (1993) Backbone-dependent rotamer library for proteins. Application to side-chain prediction. *J Mol Biol*. **230**, 543-574
- 31 Pettersen, E. F., Goddard, T. D., Huang, C. C., Couch, G. S., Greenblatt, D. M., Meng, E. C. and Ferrin, T. E. (2004) UCSF Chimera--a visualization system for exploratory research and analysis. *Journal of computational chemistry*. **25**, 1605-1612
- 32 Case, D. A., Cheatham, T. E., 3rd, Darden, T., Gohlke, H., Luo, R., Merz, K. M., Jr., Onufriev, A., Simmerling, C., Wang, B. and Woods, R. J. (2005) The Amber biomolecular simulation programs. *J Comput Chem*. **26**, 1668-1688
- 33 Hinsen, K. (2000) The Molecular Modeling Toolkit: A New Approach to Molecular Simulations. *J. Comp. Chem*. **21**, 79-85
- 34 Niesen, F. H., Berglund, H. and Vedadi, M. (2007) The use of differential scanning fluorimetry to detect ligand interactions that promote protein stability. *Nature protocols*. **2**, 2212-2221
- 35 Stupfler, B., Birck, C., Seraphin, B. and Mauxion, F. (2016) BTG2 bridges PABPC1 RNA-binding domains and CAF1 deadenylase to control cell proliferation. *Nat Commun*. **7**, 10811
- 36 Sgromo, A., Raisch, T., Backhaus, C., Keskeny, C., Alva, V., Weichenrieder, O. and Izaurralde, E. (2018) Drosophila Bag-of-marbles directly interacts with the CAF40 subunit of the CCR4-NOT complex to elicit repression of mRNA targets. *RNA*. **24**, 381-395
- 37 Garces, R. G., Gillon, W. and Pai, E. F. (2007) Atomic model of human Rcd-1 reveals an armadillo-like-repeat protein with in vitro nucleic acid binding properties. *Protein science : a publication of the Protein Society*. **16**, 176-188
- 38 Mauxion, F., Chen, C. Y., Seraphin, B. and Shyu, A. B. (2009) BTG/TOB factors impact deadenylases. *Trends Biochem Sci*. **34**, 640-647

- 39 Winkler, G. S. (2010) The mammalian anti-proliferative BTG/Tob protein family. *J Cell Physiol.* **222**, 66-72
- 40 Doidge, R., Mittal, S., Aslam, A. and Winkler, G. S. (2012) The anti-proliferative activity of BTG/TOB proteins is mediated via the Caf1a (CNOT7) and Caf1b (CNOT8) deadenylase subunits of the Ccr4-Not complex. *PLoS one.* **7**, e51331
- 41 Ezzeddine, N., Chang, T. C., Zhu, W., Yamashita, A., Chen, C. Y., Zhong, Z., Yamashita, Y., Zheng, D. and Shyu, A. B. (2007) Human TOB, an antiproliferative transcription factor, is a poly(A)-binding protein-dependent positive regulator of cytoplasmic mRNA deadenylation. *Molecular and cellular biology.* **27**, 7791-7801
- 42 Ezzeddine, N., Chen, C. Y. and Shyu, A. B. (2012) Evidence providing new insights into TOB-promoted deadenylation and supporting a link between TOB's deadenylation-enhancing and antiproliferative activities. *Molecular and cellular biology.* **32**, 1089-1098
- 43 Mauxion, F., Faux, C. and Seraphin, B. (2008) The BTG2 protein is a general activator of mRNA deadenylation. *The EMBO journal.* **27**, 1039-1048
- 44 Safaee, N., Kozlov, G., Noronha, A. M., Xie, J., Wilds, C. J. and Gehring, K. (2012) Interdomain allostery promotes assembly of the poly(A) mRNA complex with PABP and eIF4G. *Mol Cell.* **48**, 375-386
- 45 Nasertorabi, F., Batisse, C., Diepholz, M., Suck, D. and Bottcher, B. (2011) Insights into the structure of the CCR4-NOT complex by electron microscopy. *FEBS letters.* **585**, 2182-2186